International Journal of Innovative Research in Advanced Engineering (IJIRAE) ISSN: 2349-2763
Issue 09, Volume 3 (September 2016) www.ijirae.com

Point Sum Average Peak Algorithm Detection of LTE Preamble

Karthik M.S.
B.E. ECE, SSNCE

Ruthiran B.
B.E. ECE, SSNCE

Yasasvini P.
B.E. ECE, SSNCE

Abstract* — *This paper proposes an improved detection algorithm for LTE Random Access preamble detection and evaluates the performance of the algorithm with respect to the performance of algorithms proposed in the literature using MDP metric.

Keywords— detection algorithm; LTE; Random access; preamble; MDP

I. INTRODUCTION

The 3rd Generation Partnership Project (3GPP) mandates a certain access procedure for achieving synchronization between the evolved base station (eNodeB) and the mobile User Equipment (UE) in the Long Term Evolution (LTE) Standard. This Access Procedure consists of three parts, cell search which enables the UE to assess the reception quality of the current and neighbouring cells so as to conclude if a handover is necessary; transfer of system information; and Random Access. A detailed description of this access procedure is discussed in the standard [1][2][3].This Random Access procedure consists of four steps executed by the UE and eNodeB [5] that helps the network identify the UE and establish timing synchronization [Fig. 1]. The following are the four steps of Random Access,

Step 1: The UE selects one of the 64 available preambles generated from a root sequence and transmits it to the eNodeB. This preamble identifies the UE and provides Timing Advance (TA) information to the network.
Step 2: The eNodeB replies with a Random access response message that consists of a temporary identity assigned to the UE, TA information and Uplink Grant resource.
Step 3: The UE transmits a Terminal Identification message based on the temporary identity received in the previous step as part of Radio Resource Control (RRC) signaling.
Step 4: The eNodeB replies with a contention resolution message completing the RRC signaling between the network and the UE.

This Random Access Procedure also aids in transferring vital UE information to the core network in the case of a new connection setup as shown in Fig. 1.

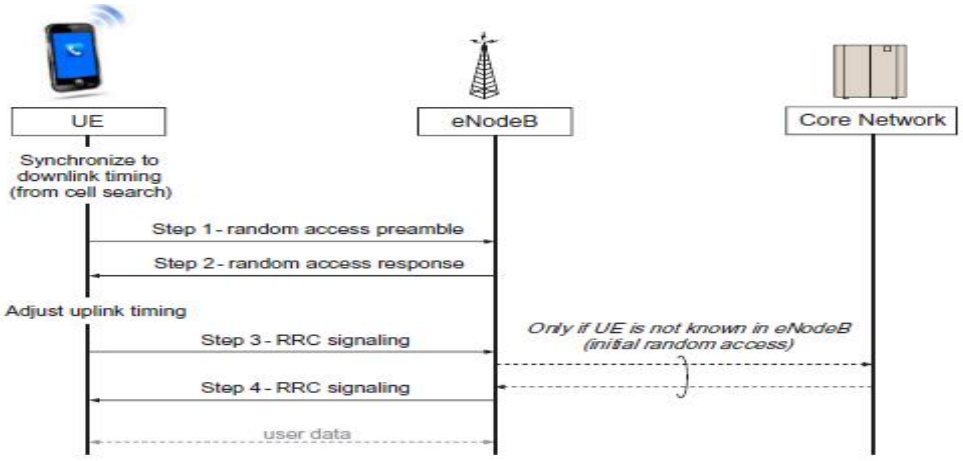

Fig. 1. Steps of Random Access [5]

The first step in this process, which is the random access preamble, needs to be correctly detected by the eNode B so as to assign the UE identity and TA information. Failing to detect this random access preamble correctly results in retransmission by the UE which could waste power and resource of the network. Initially, the preamble detection methods suggested in the literature such as Time Domain Detection and Frequency Domain Detection have been discussed in detail. Next we propose a new improved algorithm called Point Sum Average Peak (PSAP) Detection and finally, simulate these algorithms and evaluate their performance in various Rayleigh and Additive White Gaussian Noise (AWGN) channel conditions and draw inferences based on the results.

II. PREAMBLE GENERATION

The very first message of random access procedure sent by the UE to the network is basically a specific pattern or signature which is called RACH preamble. The pattern is nothing but a synchronization signal which differentiates requests coming from different UEs. There are several preamble formats, of which the Format 0 has been chosen for this implementation. The preamble format 0 is depicted in Fig. 2. The Cyclic Prefix (CP) for a symbol is obtained by copying the last few points of the symbol to the beginning of the symbol. This CP is the part of the symbol that is affected by Inter-Symbol Interference (ISI) in Orthogonal Frequency Division Multiplexing (OFDM) modulated signalling [6] and is removed at the receiver. A special signal called the Zadoff-Chu (ZC) sequence forms the preamble sequence. The Guard Period (GUARD), optional for implementation, is simply a burst period when no radio transmission can occur.

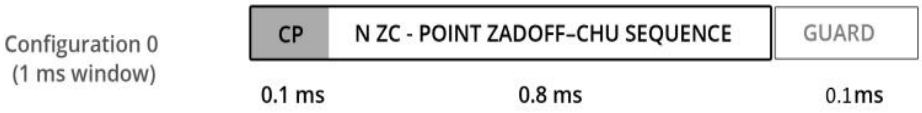

Fig. 2. Preamble Format 0

A. ZC SEQUENCE

The Zadoff-Chu (ZC) sequences are non-binary unit-amplitude sequences that are used to transmit synchronization signals such as the preamble, PSS (Primary Synchronization Signal) and the SSS (Secondary Synchronization Signal) for 3GPP LTE reference signaling[4]. They are also called the General-Chirp-Like (GCL) sequences and have excellent properties such as Constant Amplitude Zero Auto-Correlation (CAZAC) that enable them to be utilized in the 3GPP LTE standard for synchronization. A ZC sequence is a complex exponential function and can be generated by the following formula (1).

$$a_q(n) = \exp\left[-j2\Pi q \frac{\frac{n(n+1)}{2} + \ln}{N_{ZC}}\right] \quad \ldots(1)$$

where, q is the root index of the ZC sequence of length N_{ZC}. For simplicity, l is assumed to be zero for LTE applications.

B. PREAMBLE

The preamble sequences are generated from cyclic shifts of the root ZC sequence. From each ZC sequence, N_{ZC}/N_{CS} cyclically shifted sequences are obtained, where N_{CS} is the length of cyclic shift and N_{ZC} is the length of root ZC sequence. To the shifted sequence, Cyclic Prefix is appended to obtain the preamble sequence. This process is depicted in Fig 4.

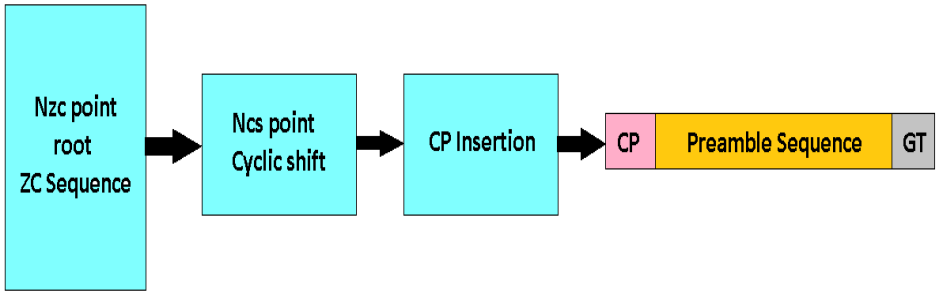

Fig. 4. Generation of Preamble from ZC sequence

DFT operation is then carried out on the preamble generated in the first step in order to reduce Peak-to-Average Power Ratio (PAPR). Then the output of DFT block is mapped onto the subcarriers, resulting in serial to parallel conversion. Then IDFT operation (equivalent to OFDM modulation) is carried out on it. DFT and IDFT are computed using FFT and IFFT respectively in order to reduce computational complexity. This process is depicted in Fig. 4.

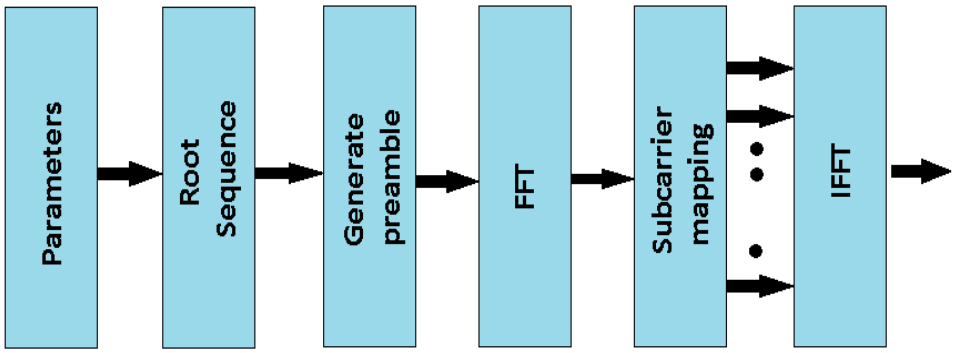

Fig. 4. Preamble Generation Block diagram

III.PREAMBLE DETECTION ALGORITHM

Generally in a multipath propagation channel, the receiver receives various taps/signals with varying power and delay, introducing ISI into the transmitted signal and thus, creating problems in detecting the correct preamble. So, in order to avoid the corruption due to ISI, cyclic prefix is used. The cyclic prefix is the portion of the symbol which gets corrupted due to copies of the previous symbols because of ISI. It is removed at the receiver.

However, the use of cyclic prefix is favoured only when the propagation delay is less than the CP length, as shown in (2). In addition to this, the noise at the receiver distorts detection peaks and Doppler shift makes the detection tough by shifting the correlation peaks into adjacent preamble window.

$$T_{Delay} \leq T_{CP} \qquad \ldots(2)$$

Where, T_{Delay} is the maximum delay introduced by the channel and T_{CP} is the duration of the CP.

The drawback of ZC sequence is the difficulty in separating frequency offset from distance dependent delay. A frequency offset results in an additional correlation peak in the time domain which corresponds to a spurious terminal-to-Base Station distance. Also, the true correlation peak is attenuated. Thus the correlation properties of the ZC sequence are rendered useless in this case.

At low frequency offsets, this effect is small and has negligible effect on the performance. However, at high Doppler frequencies, the spurious correlation peak can be larger than the true peak which results in erroneous detection of the preamble. This often forces the UE to increase the power of transmission for the preamble and retransmission. Thus it puts further pressure on the mobile UE, which has only limited power available to it.

A. TIME DOMAIN DETECTION

The detection process carried out at the receiver is the inverse of the process at the transmitter. First CP (Cyclic Prefix) and GT (Guard Time) are removed. Then, OFDM demodulation is carried out by performing DFT, followed by subcarrier demapping and IDFT. FFT and IFFT are used preferably, in order to compute DFT and IDFT for computational efficiency. After this stage, the time domain preamble sequence of length N_{ZC} is extracted. In the Correlation detection block, the root ZC sequence, which is known to the receiver, is correlated with the extracted preamble. The position of the peak of the correlated output helps in depicting the preamble used and the timing advance. Time Domain Detection method is depicted in the below Fig. 5.

Correlation operation of extracted preamble sequence, y(n) and root ZC sequence, x(n) is given by (3)

$$z(i) = \sum_{n=0}^{N_{ZC}-1} y(n)x^{*}\left[(n+1) \bmod N_{ZC}\right], i = 0,1,2.....,N_{ZC}-1 \qquad \ldots(3)$$

Where $(.)^{*}$ denotes operation of conjugate.

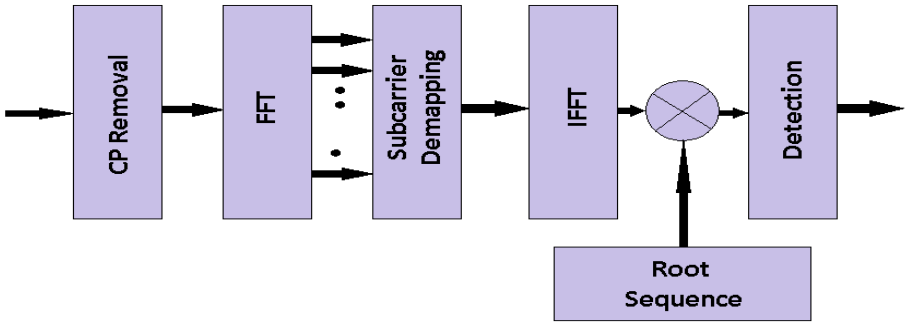

Fig. 5. TimeDomain Detection Algorithm block diagram

Correlation operation requires N_{zc}^2 number of multiplications and $N_{ZC}(N_{ZC}$ -1) number of additions. The value of N_{ZC} is chosen to be a large prime number (i.e. 839). Hence, the computational complexity of this method is very high.

B. FREQUENCY DOMAIN DETECTION

The Frequency domain detection technique is an alternative approach to identifying the preamble signature at the receiver. Computation of correlation in the frequency domain is performed before finally taking the IDFT of the sequence to find the Power Delay Profile (PDP) of the detected sequence. The block diagram of the frequency domain detection technique is depicted in Fig. 6.

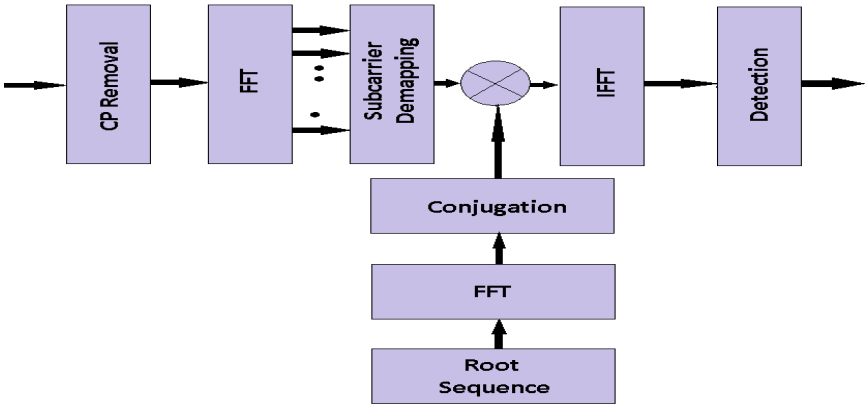

Fig. 6. Block diagram of Frequency Domain Detection of the Preamble

The cyclic prefix attached before the preamble ZC sequence is first removed, followed by guard bits if any. Then DFT operation is performed which is equivalent to OFDM demodulation. The next stage, Subcarrier De-mapping block, de-maps the ZC sequence from the subcarriers to get the frequency domain ZC sequence. Instead of performing IDFT operation directly on this frequency domain ZC sequence as is the case in time domain, the correlation block is next in the detector's implementation.

The frequency domain correlation block gives the PDP of the received signal by multiplying the received frequency domain ZC sequence with a locally generated ZC root sequence upon which the DFT operation followed by conjugation is applied. The absolute value of the conjugate multiplication product of the root and received sequence is then fed into the IDFT block which gives the PDP of the signal. [4]

The PRACH PDP calculation with the help of frequency-domain periodic correlation can be formulated as follows

$$PDP(l) = \mid Z_u \mid^2 = \left| \sum_{n=0}^{N_{ZC}-1} y(n) x^*[(n+l)N_{ZC}] \right|^2 \quad \ldots(4)$$

where Z_u is the discrete periodic correlation function at lag l of the received sequence $y(n)$ and the reference ZC sequence $x_u(n)$ of length N_{ZC} , where $(.)^*$ denotes the complex conjugate operation. Supposedly, the frequency domain implementation is computationally less complex due to its implementation with the help of radix-2 DFT and IDFT blocks that result in faster computations with lesser operations. However, the DFT operation cannot be started until the storage of the complete sequence in memory and this increases delay which is often overlooked. Also, the fact that different ZC sequences are generated from cyclic shifts of the root sequence means the frequency domain computation of the PDP of a root sequence provides in one shot the concatenated PDPs of all signatures derived from the root sequence. A computationally faster technique of detection is discussed in [12].

IV. PROPOSED ALGORITHM

The nature of noise is generally spurious in nature and hence the equally corrupted points may be spread far apart. Hence in the proximity of a noise peak, there is generally fewer noise peaks (in the correlation output). If the length of the window is considered (N_{CS}), this length is comparatively much less than the entire length of the ZC sequence and hence the possibility of multiple noise peaks lying in the same window is quite less. At the same time, considering the timing window which actually indicates the correct preamble, the noise corruption is dissimilar and diverse within the window which means the nature of the ZC sequence is maintained with a higher probability within this window. Using a point summing function within the timing window after correlation operation can factor in the underlying diversity by averaging out the peaks within the window. This technique is implemented in the frequency domain so as to take advantage of the complexity reduction due to FFT and IFFT blocks used. The block diagram of the improved algorithm is depicted in the Fig. 7. The method is quite similar to the frequency domain detection technique. The cyclic prefix and guard time are first stripped from the received preamble and the FFT operation is performed to achieve OFDM demodulation. Then, subcarrier de-mapping is done to get the N_{ZC} point ZC sequence which is the actual preamble.

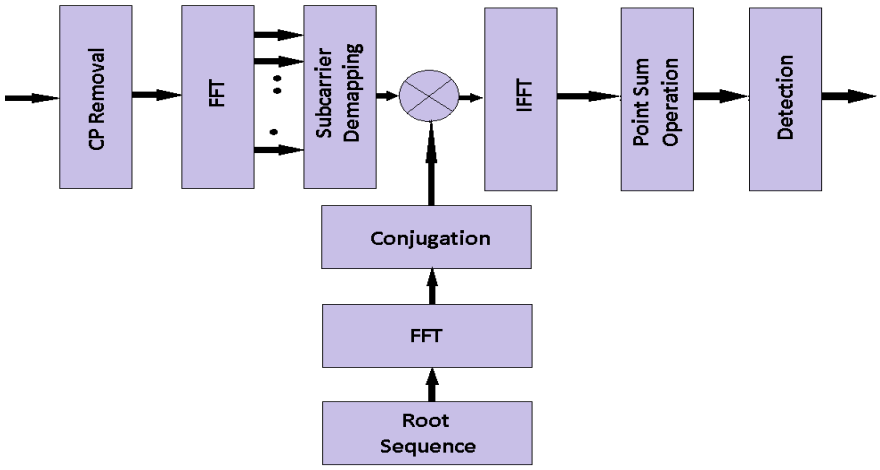

Fig. 7. Point Sum Average Peak Detection of the Preamble

The root sequence, locally known to the eNodeB is Fourier transformed in the frequency domain and the conjugate multiplication of these two sequences is performed. The resulting correlation absolute values are N_{ZC} in number. Now this correlation output is taken and divided into windows of N_{CS} length is performed. A summing operation on the points in the windows is performed and the resulting sequence has the length equal to number of preambles which is nothing but N_{ZC} / N_{CS} (here, 64). This new resulting vector is then subjected to peak detection and the position of the peak gives the preamble index and hence the identity of the transmitting UE is established. However, the detection of timing advance (TA) in this algorithm may not provide greater accuracy than the existing algorithms. The TA is calculated after identification of the preamble index by computing the delay or lag of the local maximum within the detection window (of the identified preamble) of the correlation output. This value of the TA is found to be correct up until the case where the noise peaks do not exceed the preamble correlation peak within the detection window. Beyond this, the proper detection can only be optimised. But in its defence, the network can very well handle such minor variations.

V. SIMULATION RESULTS

The various preamble detection algorithms are compared using Missed Detection Probability (MDP) for various values of Signal to Noise Ratio (SNR). The various parameters used for simulation are listed in Table I. Missed Detection Probability is defined here as the ratio of number of preambles erroneously detected to the number of preambles transmitted by the UE. The preamble index of the preamble detected at the eNodeB and that of the transmitted preamble are compared to find this probability. A similar evaluation is detailed in [8].

TABLE I - SIMULATION PARAMETERS

PARAMETERS	VALUE
SAMPLING PERIOD	130NS
DOPPLER SHIFT	200HZ
POWER DELAY PROFILE	EPA,EVA,ETU
CHANNEL	RAYLEIGH
SAMPLES	10000
BANDWIDTH	5MHZ
SUBCARRIER SPACING	15KHZ
N_{ZC}	839
N_{CS}	13

TABLE II
PDP FOR RAYLEIGH CHANNEL EPA MODEL

EXCESS TAP DELAY (NS)	RELATIVE POWER (DB)
0	0.0
30	-1.0
70	-2.0
90	-3.0
110	-8.0
190	-17.2
410	-20.8

TABLE III
PDP FOR RAYLEIGH CHANNEL EVA MODEL

EXCESS TAP DELAY (NS)	RELATIVE POWER (DB)
0	0.0
30	-1.5
150	-1.4
310	-3.6
370	-0.6
710	-9.1
1090	-7
2510	-16.9

TABLE IV
PDP FOR RAYLEIGH CHANNEL ETU MODEL

EXCESS TAP DELAY (NS)	RELATIVE POWER (DB)
0	-1.0
50	-1.0
120	-1.0
200	0.0
230	0.0
500	0.0
1600	-3.0
2300	-5.0
5000	-7.0

The Time Domain, Frequency Domain and proposed algorithms have been simulated for the Rayleigh Extended Pedestrian Model-A (EPA), Extended Vehicular Model-A (EVA) and Extended Typical Urban (ETU) Models with maximum Doppler shifts of 0 and 200Hz. The Power Delay Profile (PDP) for the three models is given in Table II, Table III and Table IV respectively. After passing the signal through the Rayleigh channel, it is further degraded by addition of AWG Noise at SNRs of -20dB to 0dB. The MDP versus SNR plots for different channel conditions for the three algorithms is plotted and depicted in Fig. 8, Fig. 9, Fig. 10, Fig. 11, Fig. 12, Fig. 13, respectively.

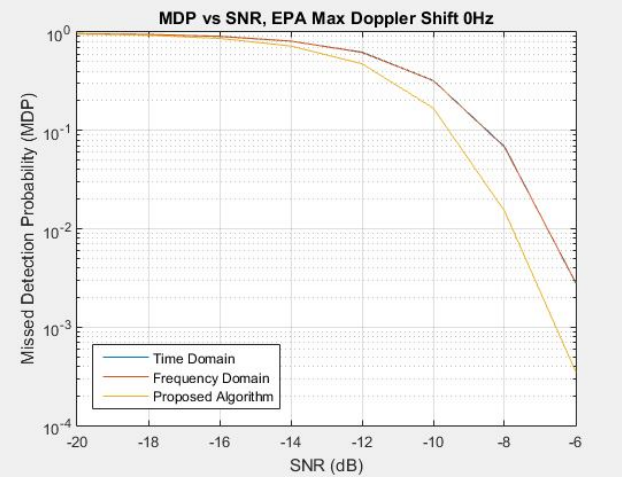

Fig. 8. MDP vs SNR for Extended Pedestrian A Model – Max. Doppler Shift 0Hz

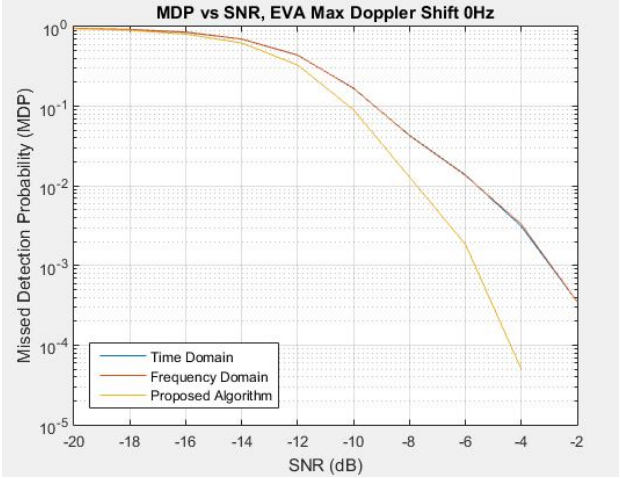

Fig. 9. MDP vs SNR for Extended Vehicular A Model – Max. Doppler Shift 0Hz

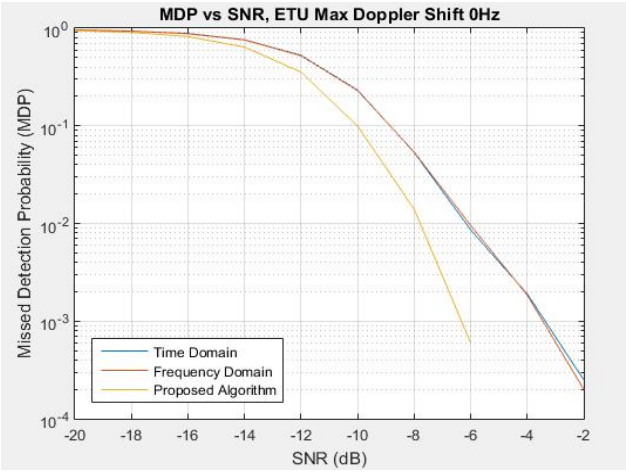

Fig. 10. MDP vs SNR for Extended Typical Urban Model – Max. Doppler Shift 0Hz

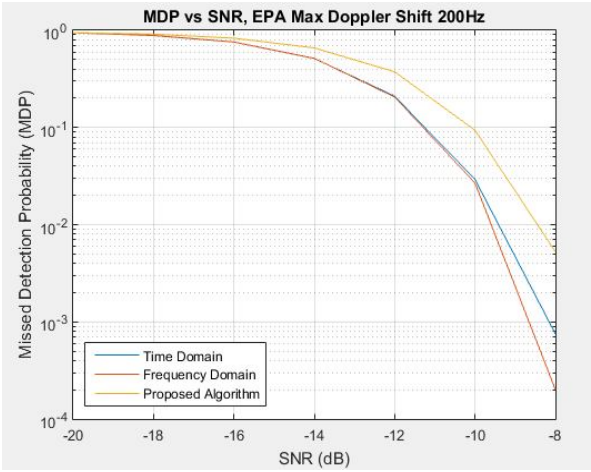

Fig. 11. MDP vs SNR for Extended Pedestrian A Model – Max Doppler Shift 200Hz

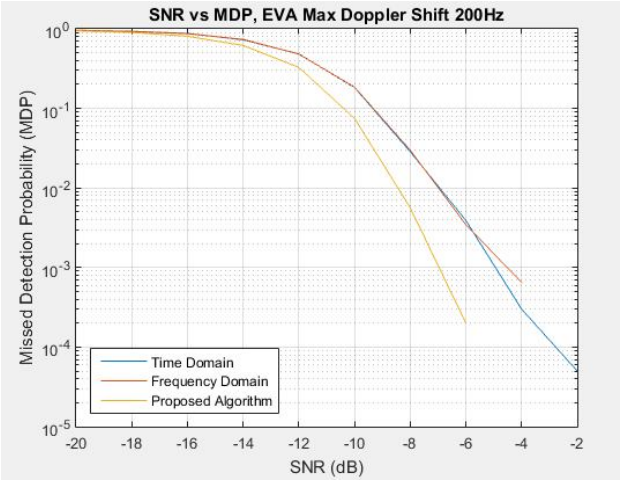

Fig. 12. MDP vs SNR for Extended Vehicular A Model – Max. Doppler Shift 200Hz

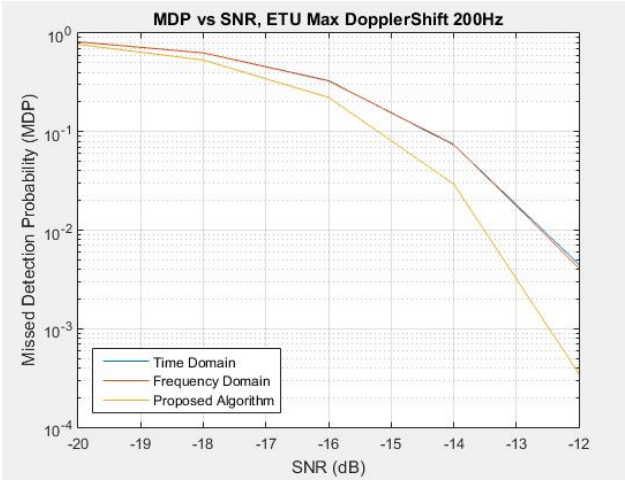

Fig. 13. MDP vs SNR for Extended Typical Urban Model – Max. Doppler Shift 200Hz

The MDP plots for varying SNR within a range of -20dB to 0dB have been plotted for each Model at a specific Doppler shift. In general, for a majority of the test scenarios, irrespective of the Rayleigh channel model used, it can be observed that the Time & Frequency Domain methods are relatively bunched together in their performance plots while the PSPA detection method starts showing significant improvement at lower to moderate SNR which is practically the case. The Rayleigh EPA model at a Doppler shift of 0Hz shows an improvement in detection efficiency for the SNR range from -12dB to 0dB (Fig. 8). The Pedestrian model is the least of the degradation models and thus almost all detection algorithms perform similarly better than in other Rayleigh channel models. In the limiting case when the degradation is minimum algorithms prescribed in the literature itself may be used. For instance as seen in Fig. 11, when Doppler shift of 200Hz is introduced into the EPA model, the proposed algorithm actually performs worse than the Time and Frequency Domain algorithms. An improved algorithm for high-speed conditions, introducing greater Doppler shifts is discussed in [9]. On the other hand, the EVA model simulation results show that the performance of the algorithms is better with and without Doppler shifts (Fig. 9 and Fig. 12 respectively). As discussed above, in the moderate to low SNR range, which is practically the case, the proposed algorithm performs better than the existing algorithms in the literature. The EVA model at a maximum Doppler shift of 200Hz results in greater interference between the various components of the ZC sequence thus leading to corruption of the nature of the sequence. But all the algorithms perform better in this case with a lesser value of MDP at relatively low SNR (-10dB). The proposed algorithm performs exceptionally well from -12dB onwards. The ETU model is used to simulate urban environment where communication is in typical metropolitan cities. The simulation results show better MDP performance by the proposed algorithm at Doppler shifts of both 0Hz and 200Hz. Also, notably, the performance in the ETU model at 200Hz Doppler shift frequency (Fig. 13) is better than the performance at 0Hz with a lower value of MDP compared to the value in 0Hz plot (Fig. 10) for the same SNR of -10dB.

In conclusion, it can be inferred that the proposed algorithm performance approaches the limiting performance of the existing algorithms at very low SNR (-20dB). But it shows significant improvement compared to all the discussed algorithms at the SNR range from -12dB to 0dB which is proof of the improvement achieved at normal operating conditions. As discussed earlier, the mobile equipment in case of very low SNR, subsequently increases the transmit power in steps and this will eventually increase the SNR leading to better detection. Hence, improvement at the normal operating conditions is more pivotal to achieving better efficiency which is what the proposed method aims for.

VI. CONCLUSION

A detailed study of preamble detection methods for 3GPP LTE standard access procedure was done. Initially, the 3GPP Release document was perused to gain an understanding of the various steps in establishing a connection and achieving synchronization between the eNodeB and the UE. The difficulty in detecting the preamble transmitted by the UE by the eNodeB was tackled by considering the different preamble detection techniques proposed in the literature as well as the modified techniques put forward in various papers [10] [11]. Consequently, the preamble generation block diagram was implemented in MATLAB software, followed by the realization of detection methods such as Time Domain detection and Frequency Domain detection. An improved technique called Point Sum Average Peak (PSAP) Detection was also proposed at this stage and also implemented in MATLAB software. Finally, these detection methods were tested in a range of Rayleigh Channel PDP conditions and for different SNR values of AWGN noise using simulations and the corresponding graphical plots were obtained. Missed Detection Probability (MDP) is the metric used to quantify the error in detection, to compare the performance of the detection of preamble at the receiver in the aforementioned conditions and inferences were drawn from these simulation plots and results detailing the working of the preamble detection techniques in each set of conditions.

ACKNOWLEDGMENT

*Our sincere thanks to, our respected Head of the Department of Electronics and Communication Engineering, SSN College of Engineering **Dr. S. Radha**, for giving us this opportunity to display our professional skills through this project. We are greatly thankful to our project guide **Dr. R. Kishore**, Associate Professor, Department of Electronics and Communication Engineering, SSN College of Engineering for his valuable guidance and motivation, which helped us to complete this project on time.*

*We would also like to express our gratitude towards **Dr. Istdeo Singh**, Domain Specialist, TATA Elxsi for providing professional guidance in shaping our project. We thank all our teaching, non-teaching staff of the Electronics and Communication Engineering department for their passionate support, for helping us to identify our mistakes and also for their constant guidance and encouragement throughout this endeavour. We heartily thank our library staff and management for their extensive support by providing the information and resources that helped us to complete the project successfully. Also, we would like to record our deepest gratitude to our parents for their constant support which encouraged us to complete our project.*

REFERENCES

[1] 3GPP, 3GPP TS 36.211 V8.6.0, Physical channels and modulation (Release 8), March 2009.
[2] 3GPP, 3GPP TS 36.212 V8.6.0, Multiplexing and channel coding (Release 8), March 2009.
[3] 3GPP, 3GPP TS 36.213 V8.6.0, Physical layer procedures (Release 8), March 2009.
[4] Stefania Sesia, Issam Toufik and Matthew Baker, 'LTE - The UMTS Long Term Evolution: From Theory to Practice', John Wiley & Sons, 2011.
[5] Erik Dahlman, Stefan Parkvall, and Johan Sköld, "4G LTE/LTE-Advanced for Mobile Broadband", Academic Press, ELSEVIER, 2011.
[6] Richard van Nee and Ramjee Prasad, "OFDM for Wireless Multimedia Communication", Artech House Universal Personal Communication Series, 2000.
[7] Yong Soo Cho, Jaekwon Kim, Won Young Yang and Chung G. Kang, "MIMO-OFDM Wireless Communications with Matlab", John Wiley & Sons (Asia) Pte Ltd, 2010.
[8] Javier López-Martínez F, Eduardo del Castillo-Sánchez, Eduardo Martos-Naya , Tomás Entrambasaguas J, 'Performance evaluation of preamble detectors for 3GPP-LTE physical random access channel', Journal of Digital Signal Processing Volume 22 Issue 3, May 2012.
[9] Liu Jinhu, Ma Jian Ting, 'Improved Algorithm of LTE Random Access Preamble Detection under the High Speed Condition', Journal of IAES, Vol 11, No 8, August 2013.
[10] Morohashi T, Koizuka A, Suzuki M and H. Morikawa, 'Inter-User Interference Cancellation Improvements for LTE-Advanced Random Access Detector using Dynamic Thresholding Mechanism' , Information and Communication Technology Convergence (ICTC), 2015.
[11] Sungbong Kim, Kyunghwan Joo and Yonghoon Lim, 'A delay-robust random access preamble detection algorithm for LTE system', in Radio and Wireless Symposium (RWS), IEEE , vol., no., pp.75-78, 2012.
[12] Alexey Fedorov, Vladimir Lyashev, Lev Rapoport, 'Fast Algorithm of LTE RACH Detection Based on Sparse Fourier Transform', Third International Conference on Digital Information, Networking and Wireless Communications (DINWC), 2015.

